Acoustic Attenuation by Two-Dimensional Arrays of Rigid Cylinders

You-Yu Chen and Zhen Ye
Wave Phenomena Laboratory, Department of Physics, National Central University, Chungli, Taiwan 32054
(Received 30 January 2001; published 15 October 2001)

In this Letter, we present a theoretical analysis of the acoustic transmission through two-dimensional arrays of straight rigid cylinders placed parallel in the air. Both periodic and completely random arrangements of the cylinders are considered. The results for the sound attenuation through the periodic arrays are shown to be in remarkable agreement with the reported experimental data. As the arrangement of the cylinders is randomized, the transmission is significantly reduced for a wider range of frequencies. For the periodic arrays, the acoustic band structures are computed by the plane-wave expansion method and are also shown to agree with previous results.

DOI: 10.1103/PhysRevLett.87.184301 PACS numbers: 43.20.+g, 42.25.Bs

When propagating through media containing many scatterers, waves will be scattered by each scatterer. The scattered waves will be scattered again by other scatterers. This process is repeated to establish an infinite recursive pattern of rescattering between scatterers, forming a multiple scattering process [1,2]. Multiple scattering of waves is responsible for a wide range of fascinating phenomena, including twinkling light in the evening sky, modulation of ocean ambient sound [3], and acoustic scintillation from fish schools [4]. On smaller scales, phenomena such as white paint, random laser [5], and electron transport in impure solids [6] are also results of multiple scattering. When waves propagate through media with periodic structures, the multiple scattering leads to the ubiquitous phenomenon of band structures. That is, waves can propagate in certain frequency ranges and follow a dispersion relation, while within other frequency regimes wave propagation is stopped. The former ranges are called allowed bands and the latter the forbidden bands. In certain situations, the inhibition of wave propagation occurs for all directions, leading to the phenomenon of complete band gaps.

The wave dispersion bands were first studied for electronic waves in solids, providing the basis for understanding the properties of conductors, semiconductors, and insulators [7]. In the late 1980s, it became known that such a wave band phenomenon was also possible for electromagnetic waves in media with periodically modulated refractive indices [8]. Since then, optical wave bands have been studied extensively, yielding a rich body of literature. The theoretical calculations matched well with the experimental observations [9].

In contrast, research on acoustic wave band structures has just started. Although theoretical computations of band structures have been documented for periodic acoustic structures [10], the experimental work was only recent, and to date only a limited number of measurements have been reported. One of the first observations was made on acoustic attenuation by a sculpture [11]. The authors obtained a sound attenuation spectrum, which was later verified by the band structure computation [12]. Recently, acoustic band structures have been further measured for acoustic transmission through two-dimensional (2D) periodic arrays of rigid cylinders placed in the air [13]. The authors demonstrated the properties of sound attenuation along two high-symmetry directions of the Brillouin zone of the arrays. They also observed a peculiar effect of deaf bands; within the bands, in spite of nonzero band states, wave propagation is prohibited due to particular symmetry of the states [13].

The main purpose of this Letter is to provide a theoretical investigation of sound transmission by 2D arrays of rigid cylinders in air in line with the experiment of [13], thus providing a direct comparison of attenuation between theory and experiment. Such a direct comparison is relatively scarce in the literature. We note that the comparison between the attenuation spectrum and the dispersion bands is of an indirect nature, as the two are not necessarily in one to one correspondence, as seen, for instance, when some seemingly allowed bands are actually deaf to wave transmission [13]. This will be further clarified in the later results. Another goal is to study how randomness affects acoustic transmission. For these purposes, we adopt a self-consistent multiple scattering theory [14].

Consider N straight cylinders located at $\vec{r}_i$ with $i = 1, 2, \ldots, N$ to form either a regular lattice or a random array perpendicular to the x-y plane; the regular arrangement can be adjusted to comply with the experiment [13]. The cylinders are along the z axis. An acoustic source transmitting monochromatic waves is placed at $\vec{r}_s$. The scattered wave from each cylinder is a response to the total incident wave composed of the direct wave from the source and the multiply scattered waves from other cylinders. The final wave reaching a receiver located at $\vec{r}_r$ is the sum of the direct wave from the source and the scattered waves from all the cylinders. Such a scattering problem can be formulated *exactly* in the cylindrical coordinates, following Twersky [14]. While the details are in [15], the essential procedure is summarized below.

The scattered wave from the jth cylinder ($j = 1, 2, \ldots, N$) can be written as

$$p_s(\vec{r},\vec{r}_j) = \sum_{n=-\infty}^{\infty} \mathrm{i}\pi A_n^j H_n^{(1)}(k|\vec{r} - \vec{r}_j|)e^{\mathrm{i}n\phi_{\vec{r}-\vec{r}_j}}, \quad (1)$$

where $\mathrm{i} = \sqrt{-1}$, $H_n^{(1)}$ is the nth order Hankel function of the first kind, and $\phi_{\vec{r}-\vec{r}_j}$ is the azimuthal angle of the vector $\vec{r} - \vec{r}_j$ relative to the positive x axis. The total incident wave around the ith cylinder ($i = 1, 2, \ldots, N; i \neq j$) is

$$p_{\mathrm{in}}^i(\vec{r}) = p_0(\vec{r}) + \sum_{j=1, j\neq i}^{N} p_s(\vec{r},\vec{r}_j), \quad (2)$$

which can be expressed again in terms of a modal series

$$p_{\mathrm{in}}^i(\vec{r}) = \sum_{n=-\infty}^{\infty} B_n^i J_n(k|\vec{r} - \vec{r}_i|)e^{\mathrm{i}n\phi_{\vec{r}-\vec{r}_i}}. \quad (3)$$

The expansion is in terms of Bessel functions of the first kind J_n to ensure that $p_{\mathrm{in}}^i(\vec{r})$ does not blow up as $\vec{r} \to \vec{r}_i$.

To solve for A_n^i and B_n^i, we express the scattered wave $p_s(\vec{r},\vec{r}_j)$, for each $j \neq i$, in terms of the modes with respect to the ith scatterer by the addition theorem for Bessel functions [16]. The resulting formula for the scattered wave $p_s(\vec{r},\vec{r}_j)$ is

$$p_s(\vec{r},\vec{r}_j) = \sum_{n=-\infty}^{\infty} C_n^{j,i} J_n(k|\vec{r} - \vec{r}_i|)e^{\mathrm{i}\phi_{\vec{r}-\vec{r}_i}}, \quad (4)$$

with

$$C_n^{j,i} = \sum_{l=-\infty}^{\infty} \mathrm{i}\pi A_l^j H_{l-n}^{(1)}(k|\vec{r}_i - \vec{r}_j|)e^{\mathrm{i}(l-n)\phi_{\vec{r}_i-\vec{r}_j}}. \quad (5)$$

The direct incident wave around the location of the ith cylinder can be expressed in a Bessel function expansion with respect to coordinates centered at $\vec{r}_i$,

$$p_0(\vec{r}) = \sum_{l=-\infty}^{\infty} S_l^i J_l(k|\vec{r} - \vec{r}_i|)e^{\mathrm{i}l\phi_{\vec{r}-\vec{r}_i}}, \quad (6)$$

with the known coefficients

$$S_l^i = \mathrm{i}\pi H_{-l}^{(1)}(k|\vec{r}_i - \vec{r}_s|)e^{-\mathrm{i}l\phi_{\vec{r}_i}}.$$

Matching the coefficients in Eq. (2), using Eqs. (3), (4), and (6), we have

$$B_n^i = S_n^i + \sum_{j=1, j\neq i}^{N} C_n^{j,i}. \quad (7)$$

At this stage, both the S_n^i are known, but both B_n^i and A_l^j are unknown. Boundary conditions will give another equation relating them. The boundary conditions state that the pressure and the normal velocity be continuous across the interface between a scatterer and the surrounding medium. After a deduction, we obtain

$$B_n^i = \mathrm{i}\pi \Gamma_n^i A_n^i, \quad (8)$$

where

$$\Gamma_n^i = \frac{H_n^{(1)}(ka^i)J_n'(ka^i/h^i) - g^i h^i H_n^{(1)\prime}(ka^i)J_n(ka^i/h^i)}{g^i h^i J_n'(ka^i)J_n(ka^i/h^i) - J_n(ka^i)J_n'(ka^i/h^i)}. \quad (9)$$

Here the primes refer to taking derivative, a^i is the radius of the ith cylinder, $g^i = \rho_1^i/\rho$ is the density ratio, and $h^i = k/k_1^i = c_1^i/c$ is the sound speed ratio for the ith cylinder.

The unknown coefficients A_n^i and B_n^j can be inverted from Eqs. (5), (7), and (8). Once A_n^i are determined, the transmitted wave at any spatial point is given by

$$p(\vec{r}) = p_0(\vec{r}) + \sum_{i=1}^{N} \sum_{n=-\infty}^{\infty} \mathrm{i}\pi A_n^i H_n^{(1)}(k|\vec{r} - \vec{r}_i|)e^{\mathrm{i}n\phi_{\vec{r}-\vec{r}_i}}. \quad (10)$$

The acoustic intensity is represented by the squared module of the transmitted wave. When the cylinders are placed regularly, we can also obtain the band structures by the plane wave method well documented in [10]. The programs used are identical to that used for computing the acoustic bands in the regular arrays of air cylinders in water [17].

Numerical computation has been carried out for experimental situations [13] and also for a random array of the cylinders. In the simulation, all the cylinders are assumed to be the same, in accordance with the experiment. Moreover, the radii of the cylinders and the lattice constants are also taken from the experiment. Several values for the acoustic contrasts between the cylinder and the air were used in the initial stage of computation. We found that the results are in fact insensitive to this factor as long as the contrasts exceed a certain value around 10. This agrees with the experimental observation. In the results shown below, we use $g = 20.69$ and $h = 17.2$ as the values for the acoustic contrasts [13]. In the computation, we allow the number of the total cylinders to vary from 100 to 500, in line with the experiment. In the particular results shown later, we assume that the cylinders are placed within a rectangular area of 8×40 of lattice domain. The source and receiver are placed about one lattice constant away from the long side of the array so as to minimize the effect due to the finite sample size. As we do not know the specifications for the transmitter and the receiver, we assume an omnidirectional transmitter as the acoustic source located on one side of the array of the cylinders, whereas an omnidirectional receiver is placed on the other side to receive the propagated waves.

In Fig. 1, we show the relative attenuation ($\sim -\ln|p|^2$) spectra for various square lattices for acoustic transmission along the [100] direction. The parameters for the four cases considered are adopted from the experiment [13]. We observe a robust attenuation peak located around 1.5 kHz for all the situation. By eye inspection of Fig. 1 and of Fig. 1 in [13], the agreement between the theoretical and the measured results is good, particularly in view of the finite dimension of the arrays and no adjustable parameters. The height of the attenuation peaks depends on the locations of either the receiver and the transmitter, on the outer boundary of the cylinder arrays, and on the number of cylinders. Nevertheless, the theoretical results describe quantitatively

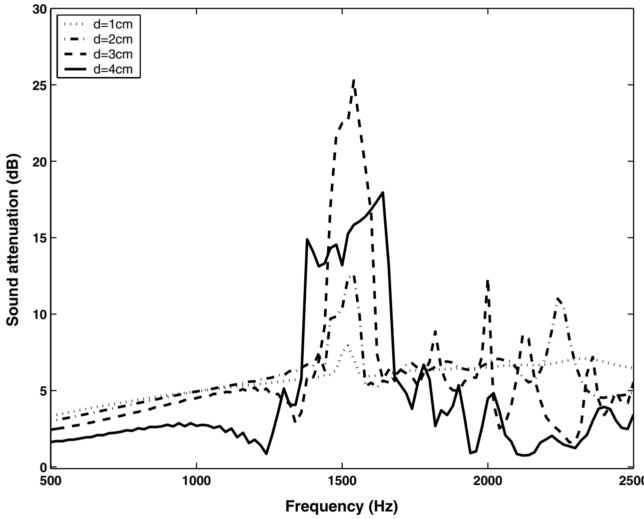

FIG. 1. Theoretical results for the relative acoustic attenuation along [100] as a function of frequency for various arrangements of cylinders. The filling factors are 0.006, 0.026, 0.058, and 0.104 for $d = 1, 2, 3, 4$ cm, respectively, taken from the experiment.

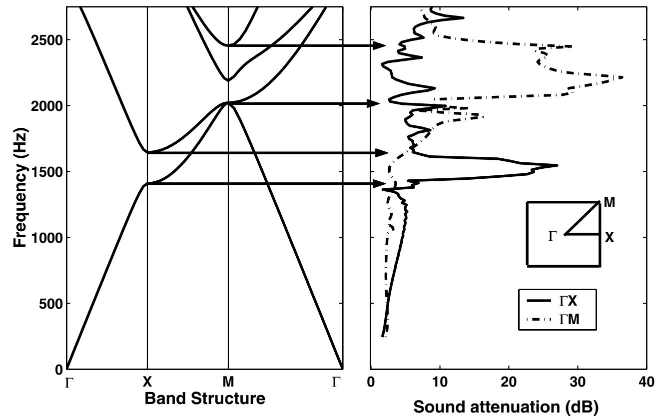

FIG. 2. Right panel: Relative acoustic attenuation vs frequency for a square array of cylinders with periodicity 11 cm. The radius of the cylinders is 3 cm. Left panel: The band structures computed by the plane-wave expansion method.

well the observation. A slight difference appears, however, for the case with cylinders of diameter 1 cm at the filling of 0.006. In our results, a small attenuation peak occurs at about 1.5 kHz, but is absent from the experiment. This discrepancy may be attributed to a couple of reasons: the theoretical setting does not match exactly that in the experiment and perhaps the attenuation peak is too small to be observable experimentally. For frequencies within the gap, the qualitative feature of the transmission is insensitive to the arrangement of the transmitter and receiver. In Fig. 1 we also observe some peaks located at higher frequencies as observed in the experiment. These peaks are sensitive to the arrangement of the transmitter and receiver, and the number of the cylinders.

Figure 2 shows the attenuation (relative) spectra for the case of cylinders of diameter 3 cm in a square lattice with lattice constant 11 cm. The corresponding band structure is also depicted. In the figure, the curves on the left denote various dispersion bands when the wave is propagating in different directions. The inserted box on the right panel denotes the Brillouin zone. For example, ΓX refers to the [100] direction, and ΓM refers to [110] direction, while XM refers to the wave vector varying from [100] to [110] on the side of the Brillouin zone.

The attenuation along the [100] and the [110] directions is represented in solid and dotted lines on the right panel, respectively. Comparing Fig. 2 with the experimental Fig. 2 in [13], we see that the attenuation peak along [100] coincides almost exactly with the experimental data in the frequency range between 1.38 and 1.70 kHz. In this particular case, the attenuation peaks are also roughly of the same order of magnitude as in the observation. Along the [110] direction, the attenuation due to the deaf bands is also nicely recovered by the theory. That is, the two bands predicted by the band structure computation (the second and the third bands in Fig. 2 for the range from M to Γ) are actually deaf and wave propagation is prohibited within these two bands. Similar results have also been reported for 2D photonic band gap materials [9,18]. Further simulation shows that, although the height of the attenuation peaks may vary as the outer boundary of the cylinder arrays changes, the overall shape of the attenuation spectra remains unchanged.

We also notice that the width of the attenuation peak along [110] is a little wider than the observation. In addition to the aforementioned reasons, this discrepancy could be due to the fact that in the present simulation the cylinders are assumed to be in the open air, while the experiment was performed in a chamber which may somewhat still reflect sound. Furthermore, the exact number and the setting of the cylinders in the experiment are also not known from the literature. Other contributions to the discrepancy may result from the different acoustic source and receiver used in the theory and experiment. In spite of these limitations, the match between the theory and experiment is quite encouraging.

The band structure shown in Fig. 2 is obtained by using the usual plane-wave method [10]. Here it is shown to agree nicely with the band structure obtained by the variation method calculation. With the parameters in Fig. 2, wave propagation in different directions is inhibited within different frequency regimes. It was suggested that the overlap of attenuation peaks along different directions, an indication of the complete band gap, can be observed when the cylinder filling factor exceeds certain values [13]. In our simulation, there is no evidence for such overlapping.

Now consider the effect of randomness on the acoustic transmission. Here we take the case described by Fig. 2 as the example. While keeping the same cylinder filling and the outer boundary of the array, we allow the cylinders to be distributed completely randomly within the area.

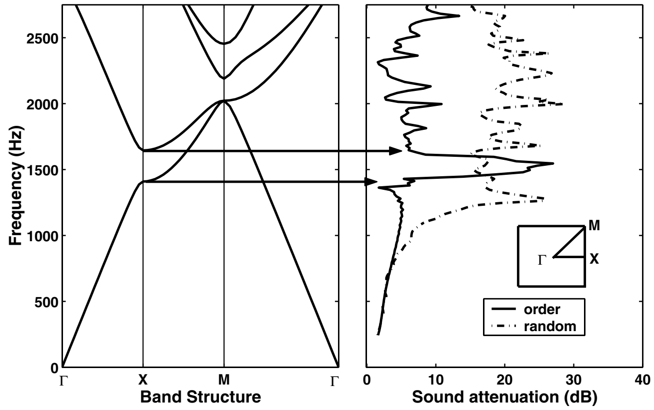

FIG. 3. The right panel shows the relative acoustic attenuation vs frequency. Here the comparison is made between the results from a square array with periodicity 11 cm (solid line) and from a complete random array of cylinders (dotted line). The radius of the cylinders is 3 cm. Left panel: Band structures computed by the plane-wave expansion method.

The relative attenuation is computed again. The results are shown in Fig. 3, with comparison to the results for wave propagation along [100] for the corresponding square latter array. The following features are evident. At low frequencies, the introduced disorder does not affect the transmission for the given size of the sample. The randomness reduces the transmission basically for all frequencies above a critical frequency of 700 Hz, except for the frequencies within the lowest stop band along [100] within which, although the transmission is still inhibited, the disorder actually reduces the attenuation purely due to the stop-band effect; such a feature is also observed in other acoustic systems [19]. As we increase the sample size, the critical frequency tends to become smaller, implying larger ranges of inhibition. Note that, in order to compute the transmission accurately at lower frequencies, larger sample sizes are required and the computation would become costly. The result of the severe reduction in transmission for a wide range of frequencies is remarkable and may be of relevance to the fundamental problem of Anderson localization [20]. The results also imply that random arrays of rigid cylinders are good candidates in filtering audible noise.

In summary, here we have applied the multiple scattering theory to study the acoustic transmission through regular arrays of rigid cylinders, yielding favorable agreements with experimental results. The theoretical results verify the existence of the deaf bands. The results are subsequently extended to the case of random cylinder arrays. We found that wave propagation is significantly reduced by randomness for a wide range of frequencies.

The help from E. Hoskinson now at UC Berkeley (Physics) is greatly appreciated. This work received support from NSC.

[1] A. Ishimaru, *Wave Propagation and Scattering in Random Media* (Oxford University Press, New York, 1997).
[2] Z. Ye, H. Hsu, E. Hoskinson, and A. Alvarez, Chin. J. Phys. **37**, 343 (1999).
[3] Z. Ye, J. Appl. Phys. **78**, 6389 (1995).
[4] Z. Ye, T. Curran, and D. Lemon, J. Mar. Sci. **53**, 317 (1996).
[5] N. M. Lawandy *et al.,* Nature (London) **368**, 436 (1994).
[6] S. Datta, *Electronic Transport in Mesoscopic Systems* (Cambridge, New York, 1995).
[7] C. Kittel, *Introduction to Solid State Physics* (John Wiley & Son, New York, 1996).
[8] E.g., E. Yablonovitch, Phys. Rev. Lett. **58**, 2059 (1987); S. John, Phys. Rev. Lett. **58**, 2486 (1987).
[9] W. Robertson *et al.,* Phys. Rev. Lett. **68**, 2023 (1992).
[10] M. S. Kushwaha, Int. J. Mod. Phys. B **10**, 977 (1996).
[11] R. Martínes-Sala *et al.,* Nature (London) **378**, 241 (1995).
[12] M. S. Kushwaha, Appl. Phys. Lett. **70**, 3218 (1997).
[13] J. V. Sánchez-Pérez *et al.,* Phys. Rev. Lett. **80**, 5325 (1998).
[14] V. Twersky, J. Acoust. Soc. Am. **24**, 42 (1951).
[15] Z. Ye, Proc. Natl. Sci. Counc., Repub. China, Part A: Phys. Sci. Eng. **25**, 135 (2001).
[16] I. S. Gradshteyn, I. M. Ryzhik, and A. Jeffrey, *Table of Integrals, Series, and Products* (Academic Press, New York, 1994), 5th ed.
[17] Z. Ye and E. Hoskinson, Appl. Phys. Lett. **77**, 4428 (2000).
[18] T. F. Krauss, R. M. de la Rue, and S. Brand, Nature (London) **383**, 699 (1996).
[19] A. R. McGurn, K. T. Christensen, F. M. Mueller, and A. A. Maradudin, Phys. Rev. B **47**, 13 120 (1993).
[20] P. W. Anderson, Phys. Rev. **109**, 1492 (1958).